Axial single-shot EPI Diffusion Tensor Imaging of the human spinal cord

C. Rossi[1,2], A. Boss[1], G. Steidle[1], P. Martirosian[1], C. D. Claussen[3], F. Schick[1]

[1]Section of Experimental Radiology, University of Tübingen, Tübingen, Germany, [2]Physics Department, La Sapienza University, Rome, Italy, [3]Department of Diagnostic Radiology, University of Tübingen, Tübingen, Germany

Purpose

Diffusion tensor imaging (DTI) of the brain provides important information for the detection of structural pathological changes of the white matter, which are not evident on the conventional images [1]. Application of DTI to the spinal cord is hampered by its need for highly resolved spatial encoding in an area of high magnetic field inhomogeneities. Until now there are several challenges that must be overcome in spinal cord DTI imaging due to the flow of the cerebrospinal fluid (CSF) around the cord, the relatively small cross-sectional dimensions of the cord with a large vertical extent and the magnetic susceptibility differences between the spinal cord and the surrounding bone structures. Several different modalities have been reported to successfully depict the spinal cord in DTI using line scan imaging, steady-state free procession, fast spin-echo, navigated echo-planar [2,3,5] or ZOOM-echo-planar [4] data readout techniques. The recent improvements in the gradient systems technology reduce the distortions and susceptibility artifacts due to eddy currents usually related with single shot EPI leading to the need for a new optimization of sequence parameters. In this study, we systematically evaluated imaging parameters in echo-planar imaging. An optimized DTI protocol with single shot EPI readout is proposed for the acquisition of axial slices of the human spinal cord.

Material and Methods

Diffusion imaging was performed on a whole-body 1.5 T MRI system (Siemens Medical Solutions, Erlangen, Germany) equipped with actively shielded magnetic field gradients unit with a maximum intensity of 45 mT/m and a maximal slew rate of 200 mT/m/ms. A single element posterior cervical spine coil was used for signal reception and the built-in body coil was used for spin excitation. Diffusion images were acquired with a double spin echo diffusion preparation and single shot EPI readout. Sequence parameters were systematically varied: b-value, matrix size, receiver bandwidth, field of view, echo-time, and positioning of saturation bars. The optimized protocol consisted of a series of 9 cervical axial slices with slice thickness of 5 mm, using two fat saturation bars and the posterior-anterior direction for phase encoding. Axial slices were necessary to reduce partial volume effects between white and gray matter signals [3,4]. The matrix size was 64x48 and the field of view (FOV) was 56x48 mm^2, leading to a nominal voxel size of 0.9x0.9x5.0 mm^3. The receiver bandwidth (BW) was 1015 Hz/pixel, the TE was 76 ms, TR was 3000 ms and the b-value was set to 700 s/mm^2. The diffusion weighted images were analyzed offline using homemade routines. A binary filter was applied to select only the spinal cord and reduce the presence of the CSF. The images were interpolated up to 256x192 pixels. The diffusion tensor was then calculated and diagonalized on a pixel-by-pixel basis and parametrical maps were calculated starting from the computed eigenvalues, D_1, D_2 and D_3. The Mean Diffusivity (MD) and the Fractional Anisotropy (FA) maps were computed offline as well.

$$MD = \frac{D_1 + D_2 + D_3}{3} \qquad FA = \frac{\sqrt{3\left[(D_1 - MD)^2 + (D_2 - MD)^2 + (D_3 - MD)^2\right]}}{\sqrt{2\left(D_1^2 + D_2^2 + D_3^2\right)}}$$

Results

The quality of the acquired images and the parametrical maps was improved by acting mainly on the BW, the TE, the matrix size and FOV with the aim of joining a higher spatial resolution with a good signal-to-noise ratio. As shown in Fig. 1, the butterfly shape of the gray matter is recognizable in each parametrical map and the FA pattern agrees with anatomical bases ($FA_{CSF} < FA_{gm} < FA_{wm}$). The FA and MD values (Tab. 1) were subsequently compared with the literature [4]. Similar values were found for the MD and FA of the white matter (w) while the gray matter (g) FA shows a significant high value (0.532±0.031) seemingly related to an axial symmetry. Such a value has to be further analyzed in order to distinguish between the partial volume effect due to the white matter and an effective axial symmetry of the tissue.

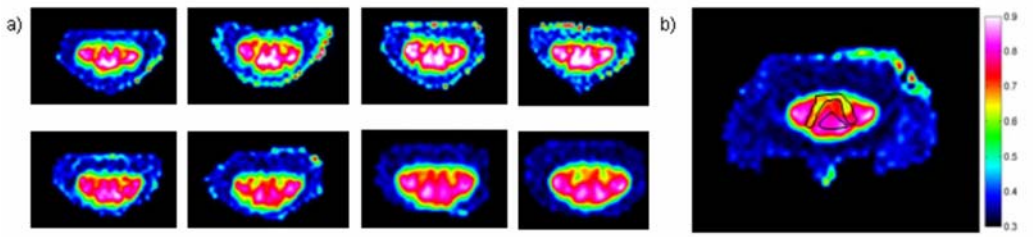

Fig. 1 The FA maps of each acquired axial slice are shown (a, b). As expected for an isotropic diffusion regime the CSF surrounding the spinal cord looks less intense while, because of the axial symmetry of the myelinated axons, the white matter looks more intense than the gray matter. In fig. 1.b) the ROIs for white and gray matter FA evaluation are traced in black.

	MD_W (10^{-6} mm^2/s)	FA_w	MD_g (10^{-6} mm^2/s)	FA_g
Rossi et al.	(813±51)	(0.784±0.040)	(810±19)	(0.532±0.031)
Wheeler-Kingshott et al. [3]	(940±40)	(0.61±0.05)	-	-

Tab. 1 The MD and the FA computed on a ROI basis are reported and compared with the published data [4]. A good agreement was found for the white matter, while no data are available for the gray matter values comparison. A further analysis of the gray matter data is necessary in order to clarify the origin of such a high FA value.

Conclusion

Using an optimized DTI protocol with a single shot EPI readout, the recent improvements in the gradient system technology lead to a distinct increase in the image quality in diffusion tensor imaging of the spinal cord. The FA maps show the characteristic butterfly shape of the gray matter with an optimal in plane resolution of 0.9x0.9 mm^2. A further analysis of the FA values, (0.532±0.031), of the gray matter will be the aim of further studies in order to clarify the origin of such a result. A further next step may be the optimization of a DTI protocol for the spinal cord at higher magnetic field (3T) possibly offering higher signal yield.

References

[1] Basser P., **NMR in Biomedicine**, 8:333-344, 1995.
[2] Clark C., et al., **NMR in Biomedicine**, 15:578-586, 2002.
[3] Ries M., et al., **Magnetic Resonance in Medicine**, 44:884-892, 2000.
[4] Wheeler-Kingshott C., et al., **NeuroImage**, 16:93-102, 2002.
[5] Xu D., et al., **Magnetic Resonance Imaging**, 22:751-759, 2004.